Communications in Physics, Vol. 33, No. 1 (2023), pp. 73-84
DOI: https://doi.org/10.15625/0868-3166/17434

Effects of hydrophobic and electrostatic interactions on the escape of nascent proteins at bacterial ribosomal exit tunnel

Bui Phuong Thuy[1,2,3,†], **Le Duy Manh**[1,2,3], **Nguyen Thi Hai Yen**[2] and **Trinh Xuan Hoang**[2,1]

[1]*Graduate University of Science and Technology, Vietnam Academy of Science and Technology, 18 Hoang Quoc Viet, Cau Giay, Hanoi 11307, Vietnam*

[2]*Institute of Physics, Vietnam Academy of Science and Technology, 10 Dao Tan, Ba Dinh, Hanoi 11108, Vietnam*

[3]*Institute of Theoretical and Applied Research, Duy Tan University, Hanoi, 100000, Vietnam*

E-mail: [†]buiphuongthuy@duytan.edu.vn

Received 19 August 2022

Accepted for publication 21 September 2022

Published 6 January 2023

Abstract. *We study the escape process of nascent proteins at the ribosomal exit tunnel of bacterial Escherichia coli by using molecular dynamics simulations with coarse-grained and atomistic models. It is shown that the effects of hydrophobic and electrostatic interactions on the protein escape at the E. coli's tunnel are qualitatively similar to those obtained previously at the exit tunnel of archaeal Haloarcula marismortui, despite significant differences in the structures and interactions of the ribosome tunnels from the two organisms. Most proteins escape efficiently and their escape time distributions can be fitted to a simple diffusion model. Attractive interactions between nascent protein and the tunnel can significantly slow down the escape process, as shown for the CI2 protein. Interestingly, it is found that the median escape times of the considered proteins (excluding CI2) strongly correlate with the function $N_h + 5.9Q$ of the number of hydrophobic residues, N_h, and the net charge, Q, of a protein, with a correlation coefficient of 0.958 for the E. coli's tunnel. The latter result is in quantitative agreement with a previous result for the H. marismortui's tunnel.*

Keywords: Post-translational escape; ribosomal exit tunnel; electrostatic and hydrophobic interactions; diffusion model.

Classification numbers: 87.15.M-; 87.64.K-.

1. Introduction

In ribosomes, protein biosynthesis takes place at the peptidyl transferase center (PTC) which is connected to the ribosomal exit tunnel. Newly synthesized proteins are released from a ribosome through the exit tunnel. The latter impacts co-translational folding [1–3] of the nascent polypeptides as well as the post-translational escape [4–7] of nascent proteins. Despite the complex shape of the ribosome tunnel and its diverse interactions with nascent chains, recent simulation studies have shown that the escape process of nascent proteins is akin to simple diffusion given by a one-dimensional diffusion model [5–7]. The protein escape time, however, can be modulated by energetic interactions of the ribosome tunnel with nascent proteins, such as hydrophobic and electrostatic interactions [7]. These energetic interactions may also increase the chance of kinetic trapping of small proteins inside the tunnel. Note that it is important for nascent proteins to escape efficiently from the exit tunnel because a too slow escape or a kinetically trapped protein would delay the ribosome cycle.

Besides certain conservations, there are notable differences in the structures of ribosomal exit tunnels among species [8]. Not only the shape but also the detailed chemistry of the ribosome tunnel can affect the escape of nascent proteins differently for different tunnels depending on specific distributions of charges and hydrophobic residues of a given tunnel. Therefore, the protein escape process must be studied for various types of ribosome tunnels.

In our previous work [7], the escape process has been studied for a number of small globular proteins at the ribosome exit tunnel of H. marismortui, an archaeon from the Halobacteriaceae family. This study shows that the hydrophobic and electrostatic interactions of the tunnel modulate the escape time in a simple way, yet do not alter the diffusional mechanism of the escape process. Specifically, the protein median escape time, $t_{\rm esc}$, was shown to strongly correlate with the function $N_h + 5.9Q$, where N_h is the number of hydrophobic residues and Q is the total charge of a protein, with a correlation coefficient exceeding 0.96. This strong correlation indicates that on average the dependence of t_{esc} on Q is ~ 6 times stronger than on N_h.

In the present work, we extend our study to the ribosomal exit tunnel of Escherichia coli bacteria in order to check whether the previous results on the protein escape process persist for this type of ribosomal tunnel. E. coli belongs to a different biological domain than H. marismortui and their exit tunnels differ significantly. To have thorough comparisons we considered the same set of proteins and employed the same coarse-grained and atomistic models for the proteins and for the tunnel as in Ref. [7], except that the structure for the ribosome tunnel has been changed to E. coli's. The system was simulated by using molecular dynamics method based on the Langevin equation of motion. We will show that besides some differences, the results on the E. coli's tunnel substantially agree with those obtained for H. marismortui.

The stages of a protein formation, from translation to complete folding, are schematically illustrated in Fig. 1. In the translation process, the ribosome is moving along a messenger RNA to translate the genetic information carried by the mRNA to the amino acid sequence of the protein. The translational initiation is signalled by the appearance of the protein's N-terminus in the exit tunnel, and is followed by the elongation of the nascent polypeptide chain. Cotranslational folding of the nascent polypeptide may take place inside and outside the exit tunnel. The translation is completed when the protein's C-terminus is released from the PTC, and is followed by the post-translational escape which proceeds until the entire protein is found outside the tunnel.

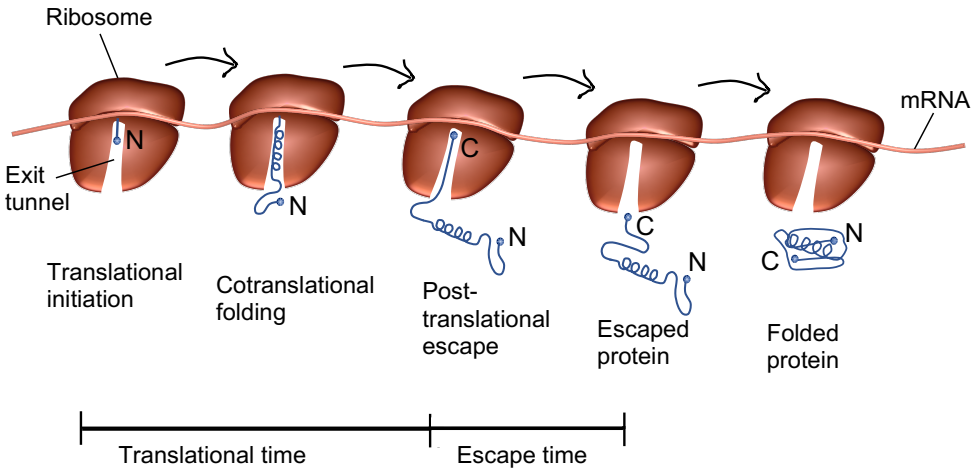

Fig. 1. Schematic illustration of the stages of a protein formation, from translation at the ribosome to complete folding outside the ribosome.

After escaping from the exit tunnel, the nascent protein continues the folding to its native state (folded protein), whereas the freed ribosome can start a new translation cycle. In this study, we investigated the escape process by simulating the progress of a protein transformation from its translational initiation to the complete escape. Note that the above picture neglects the presence of ribosome-associated chaperones and cofactors [9], which are not considered in our present study.

2. Models and methods

2.1. Tunnel model

We employ the Protein Data Bank (PDB) structure of the E.coli's large ribosome subunit with the PDB code 7k00 [10] for the tunnel model. To reduce the computational time, only atoms within a cylinder of radius $r = 45$ Å centered around an approximately chosen tunnel axis to ensure that the tunnel wall is sufficiently closed and has enough atoms for interactions with nascent proteins. As described in our previous work [7], this model retains all the heavy atoms of the ribosomal RNA, but for ribosomal proteins, only C_α atoms are considered. Amino acids in the ribosomal proteins are replaced by effective spheres of radius 2.5 Å centered at the positions of the C_α atoms. All ribosomal atoms are kept fixed during the simulations. For interactions of the tunnel with nascent proteins, we consider the three tunnel models T1, T2, T3 described in the previous work [7]. The types of interactions in these models are given briefly as follows.

T1 model

The T1 model includes only excluded volume interaction which is the repulsive potential between an amino acid residue of a nascent protein with a heavy atom or an amino acid residue of the ribosome.

T2 model

The T2 model entails the excluded volume interaction and the hydrophobic interaction. The hydrophobic interaction is given by the 10-12 Lennard-Jones potential between hydrophobic residues (Ile, Leu, Phe, Met, Val, Pro, Trp) of a nascent chain interacting with those of ribosomal proteins.

T3 model

The T3 model includes three types of interactions between the tunnel and nascent proteins: the excluded volume, the hydrophobic and the electrostatic interactions. We use the Debye-Huckel theory to describe the electrostatic interaction.

2.2. Protein model

The structure-based Gō-like model of Clementi et al. [11] is used for nascent proteins. The model considers each amino acid as a single bead at the position of the C_α atom. The energy of a native contact is given by the 10–12 Lennard-Jones potential [6], where the potential depth is a constant energy parameter for all native contacts. For each protein, the potential depth has been determined such that the folding temperature T_f, defined as the temperature of the specific heat's peak obtained by simulations, is equal to the experimental melting temperature T_m taken from literature (see Ref. [7]).

2.3. Simulation method

The motions of nascent chains were simulated by using a molecular dynamics method based on the Langevin equation of motion and the Verlet algorithm [4]. All amino acids are assumed to have the same mass, m, and the same friction coefficient ζ. We adopt an unit system such that the mass unit is m, the length unit is σ, and the energy unit is kcal/mol. σ is considered as the effective diameter of amino acids. The friction coefficient used in simulations is $\zeta = 1\ \sqrt{m\sigma^{-2}(\text{kcal/mol})}$. Given that $m = 120$ g/mol and $\sigma = 5$ Å, the simulation time is measured in the reduced units of $\tau = \sqrt{m\sigma^2/(\text{kcal/mol})} \approx 3$ ps. This time unit, appropriate for the low-friction regime, results in a very short timescale in simulations compared to the real timescale of the escape process. It has been shown that the correct timescale can be reached in simulations if one increases the friction coefficient and applies the high-friction value $\tau_H = 3$ ns for the time unit [7, 12, 13].

Each simulation starts with one amino acid, the N-terminal residue of a protein, bound to the PTC. The nascent chain then is elongated from the PTC at a constant rate with the growth time t_g per residue. For each protein, t_g must be chosen sufficiently large such that it results in converged escape properties of the protein given that the real growth times in cells are typically orders of magnitude larger than in simulations. We used $t_g = 400\tau$ for most proteins with an exception of GB1, for which larger values of t_g, up to 4000τ, were used. When the elongation is completed, the C-terminal residue is released from the PTC. The simulation is continued until the nascent protein has fully escaped the tunnel. The escape time is measured from the moment of complete elongation. All the simulations are carried out at room temperature $T = 298$ K.

2.4. Diffusion model

The diffusion model [5] considers the protein escape process as the diffusion of a Brownian particle in a one-dimensional potential field $U(x)$ with x the position of the particle. Such process is governed by the Smoluchowski equation (see [5]). Given the linear form $U(x) = -kx$ of the

external potential, where k is a constant force acting on the particle, the distribution of the escape time can be obtained from an exact solution of the Smoluchowski equation and is given by [5]

$$g(t) = \frac{L}{\sqrt{4\pi D t^3}} \exp\left[-\frac{(L - D\beta k t)^2}{4Dt}\right], \quad (1)$$

where L is diffusion distance identical to the tunnel length, D is the diffusion constant assumed to be position independent, $\beta = (k_B T)^{-1}$ is the inverse temperature where k_B is the Boltzmann constant. Interestingly, the escape time distribution in Eq. (1) can be well fitted to data from various simulations of protein escape in the Gō-like model [5–7]. It has been shown that the free energy of a protein at the ribosome tunnel is approximately linear along the escape coordinate [4, 7], which justifies the linear form of $U(x)$ in the diffusion model.

3. Results

3.1. The diffusional mechanism

It is quite clear that the shape and structure of the exit tunnel of H. marismortui and E. coli are very different [8, 14]. The difference in the shape of these two types of exit tunnels can visualize through the graph representing their effective diameter d along axis in Fig. 2. Although the effective diameter does not reflect all the information about the shape of the tunnel because of the complex, rough, and non-cylindrical surface, it also shows some differences. Fig. 2 shows that the tunnel diameter of H. marismortui is more stable than that of E. coli. Here, we are only interested in the effect of shape and energetic interactions of the tunnel on the escape of protein without considering other differences. The question is whether these differences change the escape mechanism of the proteins.

Similar to our study performed with the H. marismortui's tunnel, in this work, we also investigated the escape process of small globular proteins at the E. coli's exit tunnel at the temperature of 298K. These proteins include the B1 domain of protein G (GB1) [15], cold-shock protein (CSP) [16], the Z domain of Staphylococcal protein A (SpA) [17], the SH3 domain (SH3) [18], chymotrypsin inhibitor 2 (CI2) [19], ubiquitin (UBQ) [20], and barnase [21] (pdb codes and other properties of these proteins see Table S1 of the article [7]).

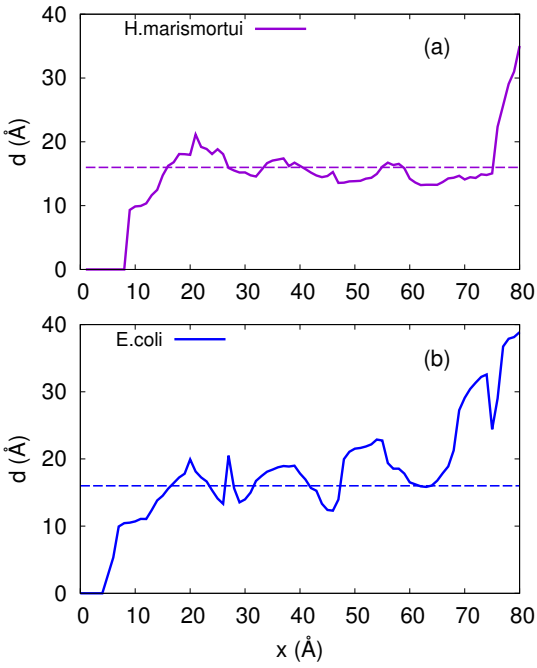

Fig. 2. The shape difference of the ribosomal exit tunnel between H. marismortui and E.coli is represented through dependence of the effective diameter d of the atomistic tunnel (solid) on x. For each position x, d is calculated as $d = 2\sqrt{(S/\pi)}$, where S is the area of the tunnel's cross section. The constant diameter $d = 16$ Å of the equivalent cylinder tunnel is indicated by the dashed line for comparison.

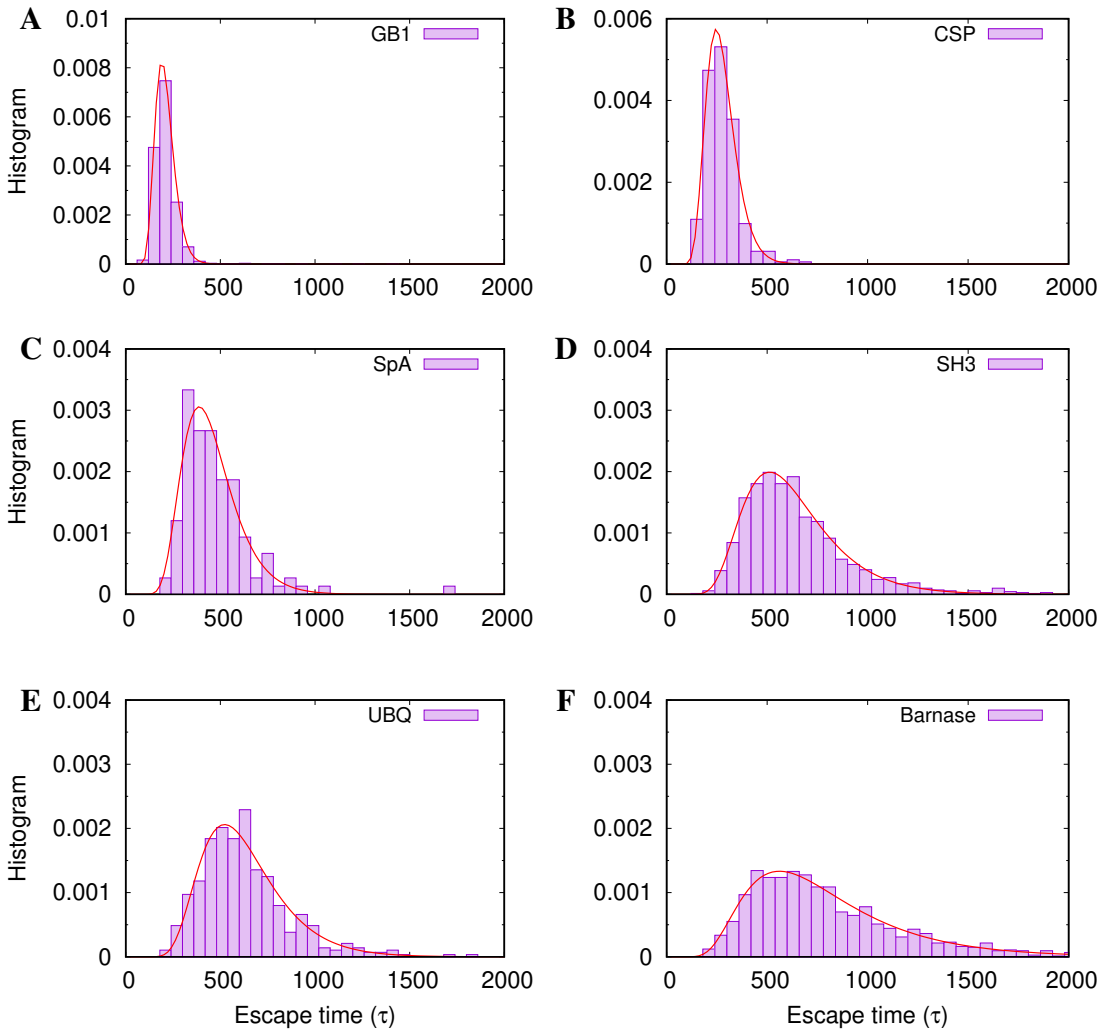

Fig. 3. Distributions of the escape time of six proteins GB1, CSP, SpA, SH3, UBQ, Barnase. The data are obtained at the temperature of $T = 298K$ at the T3 tunnel of the E. coli's ribosome.

The results show that the escape time distribution still follows the diffusion model at the E.coli's tunnel. Fig. 3 shows distributions of the escape time of 6 proteins at the T3 tunnel of the E. coli's ribosome. These distributions can fit well with the one-dimensional diffusion theory given by the Eq. 1 (red line). We also found that this agreement with diffusion theory is true for the escape of proteins at the excluded volume tunnel (T1 model). The escape of proteins is akin to a Brownian particle drift in both H. marismortui and E. coli species with and without energetic interactions. Thus, tunnel shape and energy interactions do not affect the diffusion mechanism of nascent proteins.

3.2. Effects of energetic interactions of tunnel

The dependence of the escape time on the total charge and the number of hydrophobic residues

To examine the correlation effect between hydrophobic and electrostatic interactions, we study the dependence of the median escape time, t_{esc}, at the E. coli's tunnel on the combined function $(N_h + \alpha Q)$ of the number of hydrophobic residues N_h and the total charge Q. Remarkably, the result obtained in Fig. 4 shows that the best correlation of $R = 0.985$ obtained for $\alpha = 5.9$ is similar to that of the H. marismortui's tunnel. The correlation obtained by the data of six proteins considered (excluding CI2 protein) indicates both the increases of N_h and Q cause an increase in the escape time, and the escape time depends on the total charge of protein stronger than on the number of hydrophobic residues. The optimal α-value also suggests that a change of 6 hydrophobic residues of a protein is equivalent to a change of one elementary charge in the total charge for the same effect on the median escape time. So, the dependences of the escape time on Q and N_h are quantitatively similar for the two tunnels: E. coli and H. marismortui.

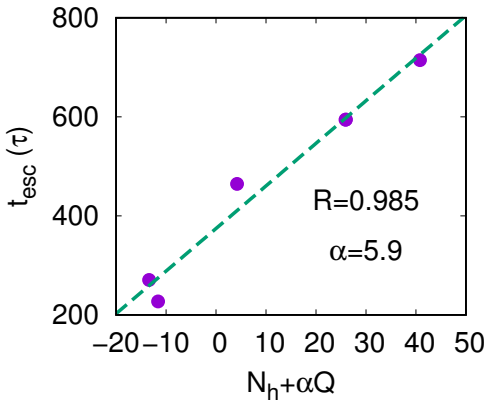

Fig. 4. Dependence of the median escape time t_{esc} on a combined function $(N_h + \alpha Q)$ of the number of hydrophobic residues N_h and the total charge Q. The best correlation of $R = 0.985$ was found for $\alpha = 5.9$. The considered proteins are GB1, SH3, SpA, CSP, UBQ, Barnase at the temperature of 298K at the T3 tunnel of the E. coli's ribosome.

Significant effects of the hydrophobic interaction of the E. coli's tunnel on the escape of CI2 protein

Although still following the diffusion theory, the escape of CI2 protein at the E. coli's tunnel with energetic interactions is much slower than those of the six proteins discussed above. Our simulation data shows that the median escape times at the T3 tunnel of the E. coli's ribosome for the six proteins considered above vary from 208τ for GB1 to 714τ for barnase. The escape times of these proteins at T3 model of the H. marismortui's tunnel vary from 234τ for GB1 to 955τ for barnase [7]. Particularly for CI2 protein, the median escape time at the E. coli's tunnel is 1459τ, much larger than that at the H. marismortui's tunnel ($t_{esc} = 818\tau$). So, the question is, what causes CI2 protein to escape more slowly than other proteins? Is it slowed down by the influence of the tunnel shape or the effect of hydrophobic or electrostatic interactions? Is it trapped in the E. coli escape?

To find out the reason for slowing down the escape of CI2, we investigated the escape process of this protein in three models of exit tunnels with and without energetic interactions. The results in Fig. 5 A, B show that CI2 escapes completely and quickly at excluded volume tunnel ($t_{esc} = 338\tau$). This escape time is about the same as that at the H. marismortui's tunnel and 4.3 times faster than that at the electrostatic tunnel of E. coli. As such, the shape of the tunnel is not the cause of the slow escape. For the T2 tunnel with the presence of the hydrophobic interaction, although CI2 protein escapes significantly more slowly, it is not trapped in the exit tunnel (Fig. 5

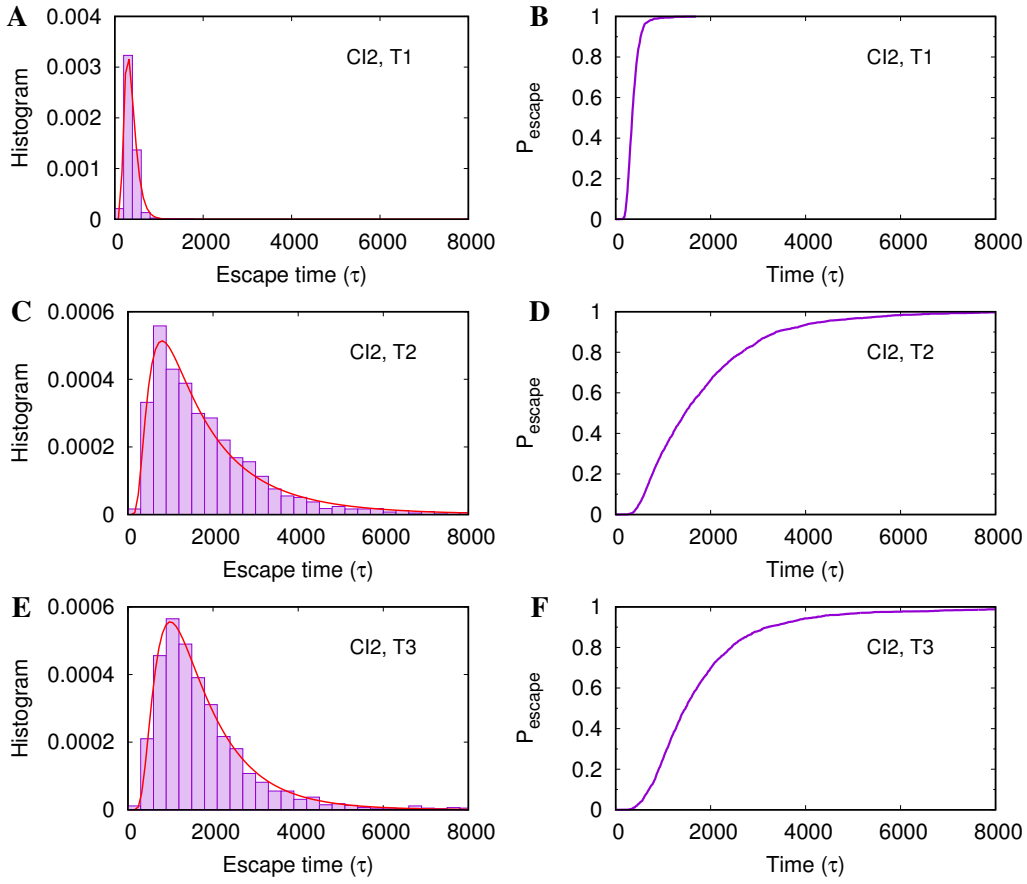

Fig. 5. Distributions of the escape time (A, C, E) and the time dependences of the escape probability P_{escape} (B, D, F) of CI2 protein for the three types of tunnel model of the E. coli's ribosome for the interactions between the tunnel and nascent proteins: the T1 tunnel with only excluded volume interaction (A and B), the T2 tunnel with excluded volume and hydrophobic interactions (C and D) and the T3 tunnel with excluded volume, hydrophobic, and electrostatic interactions (E and F). The data are obtained at the temperature of $298K$ as $t_g = 2000\tau$.

C, D). For the T3 tunnel adding the electrostatic interaction, the escape process of CI2 is very little different from that for the T2 tunnel with excluded volume and hydrophobic interactions (Fig. 5 E, F). This result indicates that the hydrophobic interaction is the leading cause of the slow release of CI2 protein and electrostatic interaction has no negligible effect on this process. The hydrophobic interaction keeps the protein from escaping slowly by the attractive force but does not trap it.

Observing the slow escape trajectories of CI2 protein, we find regions with the hydrophobic interaction between the E. coli's tunnel and the protein retarding the escape process marked in red circles (Fig. 6). It can be observed from this figure that many sites with the hydrophobic residues of CI2 match the ones along the exit tunnel surface when CI2 has completed translation and has not yet folded. The attractions of hydrophobic interactions at these sites keep CI2 in the escape

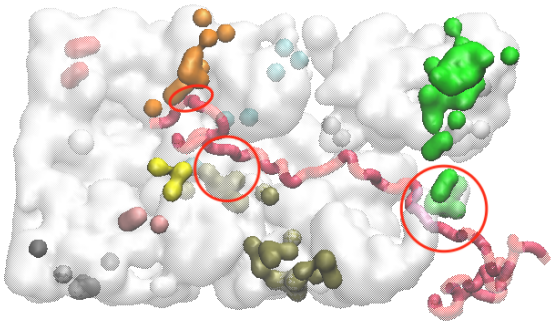

Fig. 6. The hydrophobic interactions between the E. coli's tunnel and CI2 protein slowing its escape are marked with red circles.

tunnel longer. This was not found for the other six proteins. The result found here suggests that a protein will escape slowly if there is a good match between the hydrophobic sites in the protein and on the tunnel wall.

Effects of energetic interactions of the E. coli's tunnel on the escape of GB1 protein

For GB1 protein, we found it more easily trapped in the E. coli's tunnel than in the H. marismortui's tunnel. For the H. marismortui's ribosome, at the time cut-off of 1500τ, the escape probability is 96% as $t_g = 400\tau$ [7]. For the E. coli's tunnel, this probability is only 79% with the same conditions (Fig. 7). GB1 can escape almost completely at the H. marismortui's tunnel as $t_g = 1200\tau$, whereas the escape probability is only 96% as $t_g = 4000\tau$ at the E. coli's tunnel.

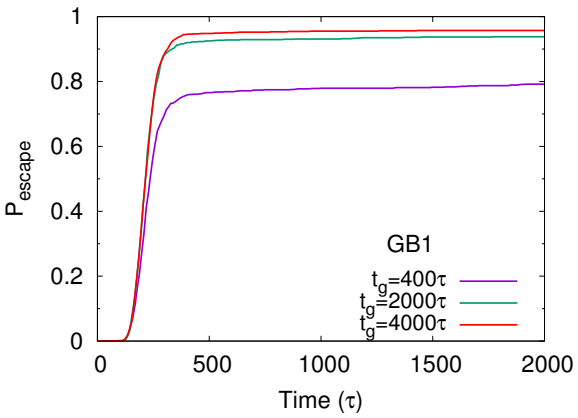

Fig. 7. (Color online) The time dependences of the escape probability P_{escape} of protein GB1 at the T3 tunnel of the E. coli's ribosome obtained with various growth time t_g per amino acid. The data are obtained at the temperature of $T = 298K$.

Figure 7 also shows that slow growth helps the protein to avoid trapping. The slowest translation speed corresponds to the growth time per amino acid $t_g = 4000\tau \approx$ 12 ns. This translational speed is faster than actual translation rates, suggesting that GB1 can still escape completely in natural conditions.

Figure 8 A, B show that the escape probability of GB1 at the T1 model of the E. coli's tunnel with only excluded volume interaction is 100%. The entrapment occurs only in the presence of

the hydrophobic and electrostatic interactions (Fig. 8 C-F). The results in Fig. 8 also indicate that GB1 escapes faster when it has energetic interactions with the E. coli's ribosome.

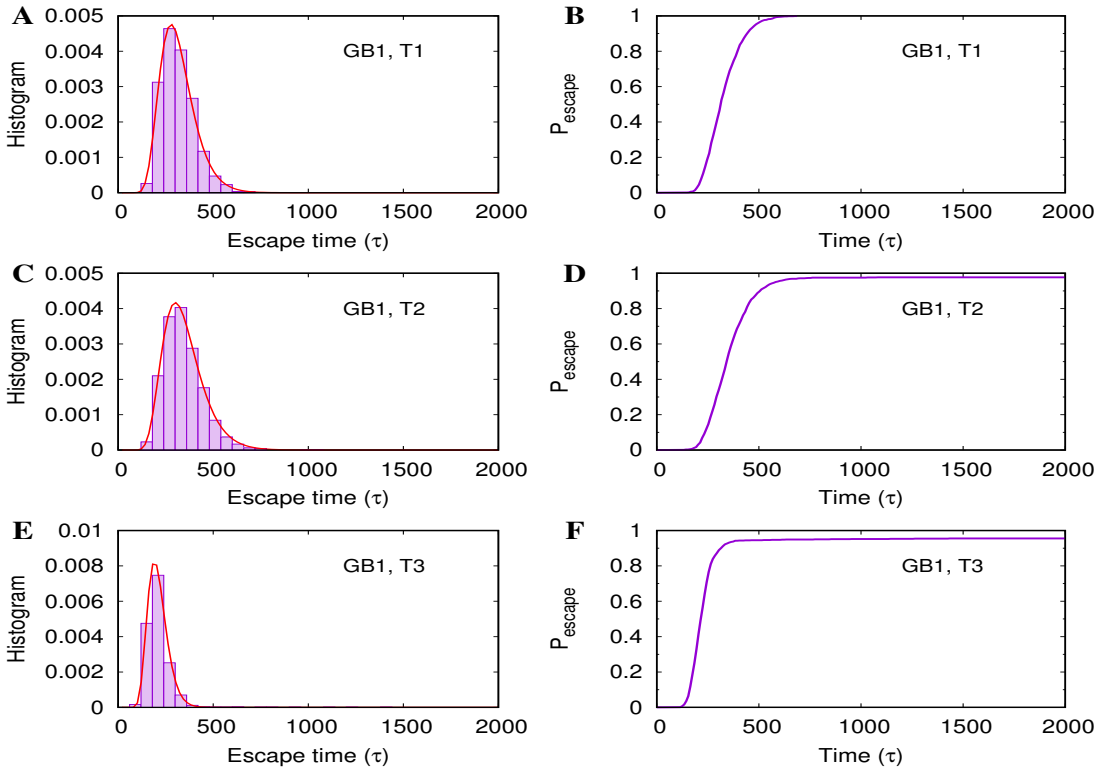

Fig. 8. Distributions of the escape time (A, C, E) and the time dependences of the escape probability P_{escape} (B, D, F) of protein GB1 for the three types of tunnel model of the E. coli's ribosome for the interactions between the tunnel and nascent proteins: the T1 tunnel with only excluded volume interaction (A and B) as $t_g = 400\tau$, the T2 tunnel with excluded volume and hydrophobic interactions (C and D) as $t_g = 4000\tau$ and the T3 tunnel with excluded volume, hydrophobic, and electrostatic interactions (E and F) as $t_g = 4000\tau$. The data are obtained at the temperature of $T = 298K$.

4. Discussion

Until now, there are no available experiment data on the protein escape times. However, the simulation results can be compared to the observed timescales of ribosome's translation cycle. It has been estimated [7] that the typical escape times are in the sub-millisecond to millisecond timescales. These timescales are much shorter than the time needed by the ribosome to translate one amino acid (tens of milliseconds), therefore not affecting the translation cycle. Kinetic trapping, however, can increase the escape time by orders of magnitude and thus can delay the cycle. The present study shows that kinetic trapping is feasible for GB1, but its probability is negligible at realistic translation rates.

In a previous study [4] of the protein escape with a cylinder tunnel, we have shown that the median escape time t_{esc} decreases with temperature like a power law. The exponent is smaller than

1 and depends on the protein and on the temperature range. For temperature $T > T_f$ (the unfolding regime) the decrease of t_{esc} with T is faster, with the exponent close to 1, than for $T < T_f$ (the folding regime). It can be expected that the dependencies of t_{esc} on T are similar in the atomistic tunnels, i.e. increasing the temperature would lead to a shorter escape time.

It is well-known that the conformation of proteins is dependent on pH and salt concentration as these factors can modify the interactions of a protein. For example, high salt concentrations can dehydrate proteins, thereby affecting their stability and promoting their aggregation. The pH can change the charges of amino acids when it goes above or below their isoelectric points, therefore proteins can be denatured at a too high or a too low pH compared to the physiological condition. For nascent proteins at the tunnel, the conformational changes due to pH or salt concentration may affect the escape time slightly towards longer escape times as folding typically promotes the escape. On the other hand, the changes of amino acids' charges due to pH, which lead to the change of the net charge of a protein, may strongly affect the escape time, as indicated by our study. It can be expected that at high pH values, the net charge of most proteins is negative, nascent proteins escape much faster than at a normal pH due to increased electrostatic repulsion by the exit tunnel. At low pH values, the net charge of most proteins is positive, nascent proteins can have a slow escape or get trapped at the tunnel.

5. Conclusions

Our study of the protein escape process at the exit tunnel of E. coli and the comparison to the escape process at the exit tunnel of H. marismortui have revealed the following similarities and differences of these processes at the two tunnels. First, for both the tunnels the complex shape as well as the energetic interactions of the tunnel do not alter the diffusional mechanism of the protein escape process, which can be elegantly described by the diffusional model as a downhill drift of a Brownian particle. Second, the strong correlations of the median escape time with the function $N_h + 5.9Q$ of the number of hydrophobic residues and the total charge of a protein are remarkably similar for the two tunnels. These similarities show that the escape process is governed by simple mechanisms which are robust against specific details of the ribosome tunnel and its energetic interactions with nascent proteins. On the other hand, the different natures of the two tunnels also lead to differences in the escape processes of specific proteins. For example, in the case of the CI2 protein, a certain good match between the hydrophobic sites in the protein and on the tunnel wall of E. coli leads to a very slow escape of this protein, whereas it is not the case for the H. marismortui's tunnel. Hydrophobic and electrostatic interactions also increase the kinetic trapping probablity of the GB1 protein at the E. coli's tunnel much more than at the H. marismortui's tunnel. However, the trapping probablity of GB1 is shown to decrease with the growth time and thus becomes negligible at realistic translation rates. Thus, besides some common properties that are conserved, the protein escape process has also some variations at the ribosomal tunnels of different species.

Acknowledgment

This research is funded by Graduate University of Science and Technology of the Vietnam Academy of Science and Technology under grant number GUST.STS.DT2020-VL03 for the postdoctoral fellowship of Phuong Thuy Bui.

Conflict of interest

The authors have no conflicts of interest to declare.

References

[1] A. N. Fedorov and T. O. Baldwin, *Cotranslational protein folding*, J. Biol. Chem. **272** (1997) 32715.

[2] D. V. Fedyukina and S. Cavagnero, *Protein folding at the exit tunnel*, Ann. Rev. Biophys. **40** (2011) 337.

[3] F. Trovato and E. P. O'Brien, *Insights into cotranslational nascent protein behavior from computer simulations*, Annu. Rev. Biophys. **45** (2016) 345.

[4] P. T. Bui and T. X. Hoang, *Folding and escape of nascent proteins at ribosomal exit tunnel*, J. Chem. Phys. **144** (2016) 095102.

[5] P. T. Bui and T. X. Hoang, *Protein escape at the ribosomal exit tunnel: Effects of native interactions, tunnel length, and macromolecular crowding*, J. Chem. Phys. **149** (2018) 045102.

[6] P. T. Bui and T. X. Hoang, *Protein escape at the ribosomal exit tunnel: Effect of the tunnel shape*, J. Chem. Phys. **153** (2020) 045105.

[7] P. T. Bui and T. X. Hoang, *Hydrophobic and electrostatic interactions modulate protein escape at the ribosomal exit tunnel*, Biophys. J. **120** (2021) 4798–4808.

[8] K. Dao Duc, S. S. Batra, N. Bhattacharya, J. H. Cate and Y. S. Song, *Differences in the path to exit the ribosome across the three domains of life*, Nucleic Acids Res. **47** (2019) 4198.

[9] J. Frydman, *Folding of newly translated proteins in vivo: the role of molecular chaperones*, Annual review of biochemistry **70** (2001) 603.

[10] Z. L. Watson *et al.*, *Structure of the bacterial ribosome at 2 angstrom resolution*, Struct. Biol. Mol. Biophys. **9** (2020) e60482.

[11] C. Clementi, H. Nymeyer and J. N. Onuchic, *Topological and energetic factors: what determines the structural details of the transition state ensemble and "en-route" intermediates for protein folding? an investigation for small globular proteins1*, J. Mol. Biol. **298** (2000) 937.

[12] T. Veitshans, D. Klimov and D. Thirumalai, *Protein folding kinetics: timescales, pathways and energy landscapes in terms of sequence-dependent properties*, Fold. Des. **2** (1997) 1.

[13] D. Klimov and D. Thirumalai, *Viscosity dependence of the folding rates of proteins*, Phys. Rev. Lett. **79** (1997) 317.

[14] A. S. Petrov *et al.*, *Evolution of the ribosome at atomic resolution*, Proc. Natl. Acad. Sci. USA **111** (2014) 10251–10256.

[15] P. Alexander, J. Orban and P. Bryan, *Kinetic analysis of folding and unfolding the 56 amino acid igg-binding domain of streptococcal protein g*, Biochem. **31** (1992) 7243.

[16] H. Welte, T. Zhou, X. Mihajlenko, O. Mayans and M. Kovermann, *What does fluorine do to a protein? thermodynamic, and highly-resolved structural insights into fluorine-labelled variants of the cold shock protein*, Sci. Rep. **10** (2020) 1.

[17] A. Myrhammar, D. Rosik and A. E. Karlström, *Photocontrolled reversible binding between the protein a-derived z domain and immunoglobulin g*, Bioconjugate Chem. **31** (2020) 622.

[18] Y.-J. Chen *et al.*, *Stability and folding of the sh3 domain of bruton's tyrosine kinase*, Proteins: Struct. Funct. Bio. **26** (1996) 465.

[19] S. E. Jackson and A. R. Fersht, *Folding of chymotrypsin inhibitor 2. 1. evidence for a two-state transition*, Biochem. **30** (1991) 10428.

[20] D. Morimoto *et al.*, *The unexpected role of polyubiquitin chains in the formation of fibrillar aggregates*, Nat. Comm. **6** (2015) 6116.

[21] J. W. Bye, N. J. Baxter, A. M. Hounslow, R. J. Falconer and M. P. Williamson, *Molecular mechanism for the hofmeister effect derived from nmr and dsc measurements on barnase*, ACS Omega **1** (2016) 669.